

Feshbach resonances in the exit channel of the $F + CH_3OH \rightarrow HF + CH_3O$ reaction observed using transition-state spectroscopy

Marissa L. Weichman¹, Jessalyn A. DeVine¹, Mark C. Babin¹, Jun Li^{2*}, Lifan Guo³, Jianyi Ma³, Hua Guo⁴ and Daniel M. Neumark^{1,5*}

The transition state governs how chemical bonds form and cleave during a chemical reaction and its direct characterization is a long-standing challenge in physical chemistry. Transition state spectroscopy experiments based on negative-ion photodetachment provide a direct probe of the vibrational structure and metastable resonances that are characteristic of the reactive surface. Dynamical resonances are extremely sensitive to the topography of the reactive surface and provide an exceptional point of comparison with theory. Here we study the seven-atom $F + CH_3OH \rightarrow HF + CH_3O$ reaction using slow photoelectron velocity-map imaging spectroscopy of cryocooled CH_3OH^- anions. These measurements reveal spectral features associated with a manifold of vibrational Feshbach resonances and bound states supported by the post-transition state potential well. Quantum dynamical calculations yield excellent agreement with the experimental results, allow the assignment of spectral structure and demonstrate that the key dynamics of complex bimolecular reactions can be captured with a relatively simple theoretical framework.

Since the development of crossed molecular beam experiments in the 1960s^{1,2}, studies of reaction dynamics via reactive scattering experiments and accompanying theoretical advances have led to major insights into the fundamental interactions that govern chemical reactivity³. A key concept in chemistry is that during the course of a reactive collision, chemical bond formation and cleavage occur in the transition-state (TS) region of the potential energy surface (PES)^{4–6}. Hence, there is much interest in characterizing the reaction TSs experimentally and theoretically⁷.

Increasingly sophisticated scattering experiments that involve state-selective reactant preparation and state-resolved product detection provide new ways to observe properties of the TS—such as the reaction barrier height and geometry—that dictate the mode specificity and the most favourable reactant orientation to promote a reactive collision^{8–10}. However, such experiments do not probe the TS region of the PES directly. Complementary experiments based on negative-ion photodetachment yield a vibrationally resolved structure characteristic of the TS¹¹, and have been applied with considerable success to benchmark bimolecular¹² and unimolecular^{13,14} reactions.

Here we report a joint high-resolution photoelectron imaging and theoretical quantum dynamics study of the $F + CH_3OH \rightarrow HF + CH_3O$ hydrogen-abstraction reaction, based on the photodetachment of the stable CH_3OH^- anion. The spectra are obtained via slow photoelectron velocity-map imaging of cryogenically cooled anions (cryo-SEVI)^{15–17}, which yields photoelectron spectra of complex species with a kinetic-energy resolution as high as 1 cm^{-1} (refs 18,19). The resolution of the cryo-SEVI spectra of CH_3OH^- and CH_3OD^- is substantially improved over previous photodetachment experiments^{20,21}; it reveals low-frequency progressions assigned to the exit-channel-bound states and Feshbach

resonances and provides new insights into the TS region of this polyatomic reaction. The experimental spectrum is assigned with the help of reduced-dimensional quantum dynamical calculations on a global PES determined by fitting a large number of high-level *ab initio* points in full dimensionality.

Dynamical Feshbach resonances of the type probed here are transient metastable states supported by the reactive PES. These resonances have sufficient vibrational energy to dissociate, but decay slowly because of the inefficient energy flow from the excited modes to the reaction coordinate. Quantum-scattering calculations indicate that the energies and widths of these resonances are exquisitely sensitive to the topography of the reactive PES^{9,12,22}. Dynamical resonances can strongly mediate reactivity and can manifest as peaks in the integral or differential cross-section as a function of collision energy^{23–26}. These effects have been sought out and, in some cases, clearly observed in molecular beam reactive scattering experiments^{9,26–30}.

Anion photoelectron TS spectroscopy offers an alternative and often more direct means to detect dynamical resonances^{11,12}. In such an experiment, a bound anion similar in geometry to the neutral TS is photodetached. The vibrational wavefunction of the anion is vertically projected onto the neutral PES, and the kinetic energy of the nascent photoelectron reports on the wave-packet evolution under the influence of the neutral Hamiltonian. The resulting photoelectron spectrum may show a broad structure if the photodetachment accesses a repulsive Franck–Condon region of the neutral PES. However, direct detachment to discrete bound or quasi-bound neutral states will manifest as sharp, well-defined features in the photoelectron spectrum³¹. These features provide valuable information on the neutral PES in strongly interacting regions, such as reactive intermediate wells and TSs. Resonances identified

¹Department of Chemistry, University of California, Berkeley, California 94720, USA. ²School of Chemistry and Chemical Engineering, Chongqing University, Chongqing 401331, China. ³Institute of Atomic and Molecular Physics, Sichuan University, Chengdu, Sichuan 610065, China. ⁴Department of Chemistry and Chemical Biology, University of New Mexico, Albuquerque, New Mexico 87131, USA. ⁵Chemical Sciences Division, Lawrence Berkeley National Laboratory, Berkeley, California 94720, USA. *e-mail: jli15@cqu.edu.cn; dneumark@berkeley.edu

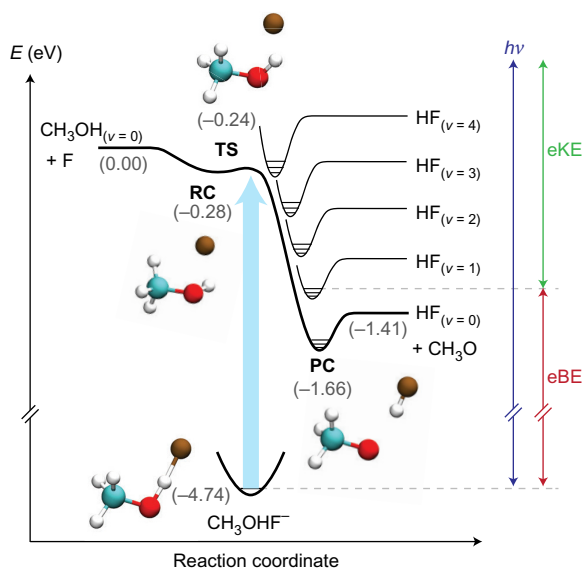


Figure 1 | Schematic energy diagram for the photodetachment of the CH_3OHF^- anion to the neutral $\text{F} + \text{CH}_3\text{OH} \rightarrow \text{HF} + \text{CH}_3\text{O}$ reactive PES. The upper bold line is the ZPE-corrected surface that connects the reactants and products in their ground vibrational states, and the curves sketched above it are the product-well HF stretching VAPs. The lower bold line represents the bound anion potential. Geometries are shown for the anion, RC, TS and PC stationary points; C, blue; O, red; H, white; F, brown. Energies derived from the fitted PIP-NN surface, shown in grey text, are given in electronvolts relative to the reactant asymptote. The relationship between the photon energy ($h\nu$), eBE and electron kinetic energy (eKE) in a SEVI experiment is also indicated.

in studies of TS spectroscopy offer an exceptional point of comparison with quantum theory, which can provide assignments based on the nodal structure of the resonance wavefunctions. Thus far, such comparisons have been limited to triatomic^{12,32,33} and tetraatomic³⁴ systems, and the somewhat irregular structure in the entrance channel of the $\text{F} + \text{CH}_4$ reaction³⁵.

Here we exploit the high resolution of cryo-SEVI spectra to observe and identify dynamical resonances in the more complex seven-atom $\text{F} + \text{CH}_3\text{OH}$ hydrogen-atom abstraction reaction. This reaction can proceed either at the hydroxyl or the methyl site, and leads to methoxy (CH_3O) or hydroxymethyl (CH_2OH) radical products, respectively. The methoxy and hydroxymethyl pathways are exothermic by 1.357(4) and 1.767(4) eV, respectively³⁶, and both are predicted to proceed without a barrier^{37–39}. The $\text{F} + \text{CH}_3\text{OH}$ branching ratio for abstraction from the hydroxyl group is considerably higher than the value of 25% expected if the branching were statistical^{38–44}. This is attributed to the fact that the hydroxyl-group abstraction proceeds through a reactant complex (RC) and TS stabilized by hydrogen-bonding interactions³⁷. The hydrogen-bonded CH_3OHF^- anion is similar in geometry to the hydroxyl-abstraction TS^{20,21,45–47}, as shown schematically in Fig. 1; further details on the calculated reactive surface are given in Results. This system is an ideal case for TS spectroscopy, but simultaneously poses a challenge, particularly to theory, with 15 degrees of freedom potentially involved in the dynamics.

Results

Experimental cryo-SEVI spectra of CH_3OHF^- and CH_3ODF^- are shown in Fig. 2b,c. The spectra are dominated by broad steps (labelled *a*, *b*, *c*, *d*, *e*), with an *a*–*b* spacing of $\sim 3,600\text{ cm}^{-1}$ in the CH_3OHF^- spectrum and $\sim 2,700\text{ cm}^{-1}$ for the CH_3ODF^- spectrum. These features were also seen in the lower-resolution photoelectron spectroscopy results of Bradforth *et al.*²⁰ and in a recent photoelectron–photofragment coincidence study by Ray *et al.*²¹ Both

prior studies assigned this stepped structure to an HF stretching progression of the $\text{CH}_3\text{O}-\text{HF}$ product complex (PC). The considerably higher spectral resolution afforded by cryo-SEVI reveals an additional layer of vibrational structure not seen previously. We now resolve a much finer structure spaced by $\sim 200\text{ cm}^{-1}$ superimposed on the broad steps with typical peak widths of $75\text{--}125\text{ cm}^{-1}$ (full-width at half-maximum (FWHM)). Peak positions and spacings are listed in Supplementary Tables 1 and 2. A key trend is that the spacing of resonances within each step increases with increasing HF stretching excitation. For example, the *a1*–*a2*, *b1*–*b2*, *c1*–*c2* and *d1*–*d2* gaps are measured experimentally as 192, 248, 255 and 315 cm^{-1} , respectively.

Accurate quantum dynamical studies on a reactive PES are necessary to interpret the experimental spectra. We model the $\text{F} + \text{CH}_3\text{OH}$ reaction using a full 15-dimensional (15D) PES constructed with $\sim 121,000$ points calculated at the explicitly correlated unrestricted coupled cluster level with singles, doubles and perturbative triples⁴⁸ with the augmented correlation-consistent polarized valence double zeta basis set and core electrons frozen (FC-UCCSD(T)-F12a/AVDZ). The CCSD(T)-F12/AVDZ method is expected to yield results of a quality comparable to that of the conventional CCSD(T)/AVQZ level. The PES is fit using the permutation invariant polynomial–neural network (PIP-NN) method⁴⁹.

Figure 1 shows a schematic of the $\text{F} + \text{CH}_3\text{OH} \rightarrow \text{HF} + \text{CH}_3\text{O}$ reaction path. The upper bold line is the zero-point energy (ZPE) corrected minimum energy path that connects the reactants and products in their ground vibrational states. The reported stationary point energies derived from the PIP-NN PES are in good agreement with prior work (Supplementary Fig. 1 gives a detailed comparison)^{21,37}. The TS, RC and PC all lie below the energy of the free reactants. The RC is a covalent three-electron two-centre hemi-bonded complex, similar to that between F and H_2O (ref. 50), which is bound by 0.28 eV relative to the free reactants, but lies only slightly lower in energy than the TS. The PC is a hydrogen-bonded complex between HF and the methoxy radical bound by 0.25 eV relative to the free products. The stationary point geometries are consistent across different levels of theory and agree well with the available experimental results (Supplementary Figs 2 and 3). The corresponding harmonic frequencies of these stationary points are compared in Supplementary Table 3.

To simulate the photoelectron spectrum, wave-packet-based quantum dynamics were investigated with a reduced 6D model by freezing the methyl moiety. The CH_3OHF^- detachment spectrum simulated with a $\sim 200\text{ fs}$ wave-packet propagation is given in Fig. 2a and compares favourably with the experimental results. The electron-binding energy (eBE) of the bottom of the PC well is calculated to lie at $24,810\text{ cm}^{-1}$, close to the experimental onset of the structure at $25,058(25)\text{ cm}^{-1}$ (peak *a1*) and to previous measurements^{20,21}. The simulated spectrum has therefore been shifted to a higher eBE by 250 cm^{-1} , so that the onset of the structure at a low eBE matches that observed experimentally. Experimental and theoretical peak positions are compared for the CH_3OHF^- detachment in Supplementary Table 1; the theory reproduces the trend of increasing resonance peak spacings mentioned above.

The product asymptote for the $\text{F} + \text{CH}_3\text{OH} \rightarrow \text{HF} + \text{CH}_3\text{O}$ reaction lies at $26,820\text{ cm}^{-1}$, while the reactant asymptote lies at $38,220\text{ cm}^{-1}$ on the ZPE-corrected PIP-NN surface. These asymptotes are marked in Fig. 2a with filled circle and diamond symbols, respectively, and have also been shifted to higher eBE by 250 cm^{-1} for comparison with the experiment. The energies of these asymptotes indicate that much of the observed structure can lie only in the PC well. The peaks in the *a* manifold fall below the product asymptote and are thus bound with respect to free HF + CH_3O products. Ray *et al.*²¹ accordingly found that the *a* manifold was associated with the production of non-dissociating neutral complexes, whereas the higher-lying peaks were correlated largely with

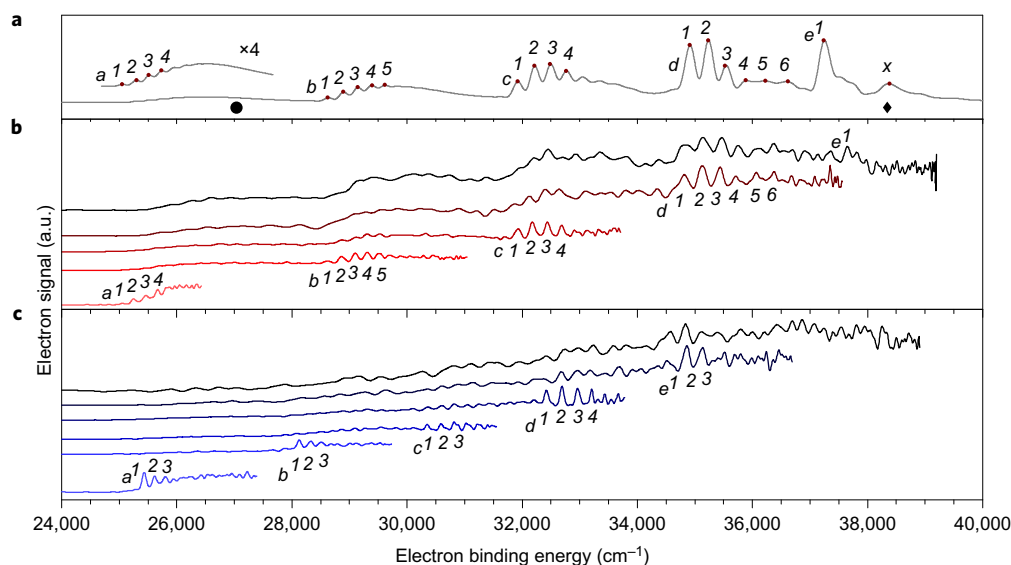


Figure 2 | Experimental and theoretical photodetachment spectra of CH_3OHF^- and CH_3ODF^- showing transitions to resonances in the $\text{F} + \text{CH}_3\text{OH} \rightarrow \text{HF} + \text{CH}_3\text{O}$ product well. **a**, Theoretical simulation of the CH_3OHF^- photoelectron spectrum obtained with an estimated 200 fs propagation time (grey). **b,c**, Experimental cryo-SEVI spectra of CH_3OHF^- (**b**) and CH_3ODF^- (**c**) detachment. The experimental overview spectra are plotted in black and the high-resolution traces taken at progressively lower photon energies are plotted in colour. The filled circle and filled diamond symbols represent the PIP-NN product and reactant asymptotes, respectively. In all the panels, the broad steps *a*–*e* represent transitions to the PC states with increasing HF stretching vibrational excitation. The numbered features associated with each step represent resonances supported by the HF(DF) stretching VAPs (see Fig. 1) with increasing CH_3O –HF stretching excitation. a.u., arbitrary units.

dissociated fragments. The agreement of experiment and theory unambiguously identifies the newly resolved low-frequency progressions as derived from discrete bound states and Feshbach resonances on the product side of the TS.

Discussion

The presence of the low-frequency progressions and the trend of their increasing spacing within steps *a*–*d* can be explained intuitively with reference to the vibrational adiabatic potentials (VAPs) shown in Fig. 1. These VAPs correspond to the HF vibrational levels plotted along the reaction coordinate and correlate to vibrationally excited free $\text{HF}(\nu) + \text{CH}_3\text{O}$ products. The HF vibrational adiabaticity is expected to be strong because of its high vibrational frequency, which couples weakly with the dissociation coordinate. Each spectral step *a*–*e* represents a detachment to an $\text{HF}(\nu = 0\text{--}4)$ VAP. The finely spaced progressions within each step are resonances supported in the wells of the VAPs and reflect increasing quanta of excitation in the low-frequency CH_3O –HF stretching mode. The VAP wells deepen as the HF excitation is increased, resulting in more widely spaced states within each well. The deepening of the PC VAPs can be explained by dynamical vibrational bonding. It is a well-known phenomenon in heavy–light–heavy^{51–53} and other triatomic^{9,54} systems that VAPs can support increasingly stabilized wells as the vibrationally excited light atom is more delocalized between the two outer fragments.

To better understand the vibrational character of the observed spectral features, the simulated wavefunctions of all the peaks were extracted. Relevant examples are shown in Fig. 3. From the localized character of these wavefunctions, it is clear that they are stable bound states or metastable resonances supported by the PC well. The $\sim 100\text{ cm}^{-1}$ FWHM peak widths of the observed spectral features allow us to place a lower bound of 50 fs on the lifetimes of the Feshbach resonance states that lie above the $\text{HF} + \text{CH}_3\text{O}$ dissociation limit, although the highest-resolution theoretical results suggest that these states are much longer lived. The final dissociation of these resonance states is expected to proceed via vibrational pre-dissociation facilitated by energy flow from

the HF stretching coordinate to translational motion along the dissociation coordinate. The large frequency mismatch means that such an energy flow is expected to be slow and result in long lifetimes for these resonances. Similar long-lived Feshbach resonance states were observed in $\text{F} + \text{H}_2\text{O}$ (ref. 34) and this picture holds even in the presence of many degrees of freedom for the $\text{F} + \text{CH}_3\text{OH}$ system.

Vibrational assignments can be confirmed by examining the resonance wavefunction nodal structure. Peaks in the *a1*–*b1*–*c1*–*d1*–*e1* progression show an increasing integer number of nodes along the HF stretching coordinate (vertical axis in Fig. 3). Therefore, the broad shelves in the spectrum indeed correspond to a progression of the HF stretching vibrational states of the PC. The isotope effect observed in the CH_3ODF^- cryo-SEVI spectrum (Fig. 2c) further validates this assignment. The increasing number of nodes in the *a1*–*a2*–*a3* progression along the CH_3O –HF coordinate (horizontal axis in Fig. 3) confirms that the finely spaced progressions are resonances with increasing quanta of excitation in the stretching mode between the product fragments. The experimental and theoretical Franck–Condon factors increase along with HF stretching excitation, as the PC vibrational states with higher quanta of excitation in the HF stretch have more wavefunction density at a larger HF displacement. Compare, for instance, the vibrational wavefunctions for peaks *a1* and *d1*: the latter has a substantially better Franck–Condon overlap with the anion wavefunction, which leads to an increased intensity in the photoelectron spectrum.

To illustrate the evolution of these resonances further, a simulated photoelectron spectrum is shown in Supplementary Fig. 4 for three different propagation times. The low-resolution spectrum obtained in the first 40 fs of propagation suggests that the short-time dynamics on the neutral PES are along the HF vibrational coordinate, as the spectrum clearly resolves peaks related to the HF vibrational frequency. By 200 fs, the fine-structure peaks emerge because of the recursion of the wave packet along the CH_3O –HF dissociation coordinate. By 800 fs, the fine-structure peaks split further into sharper peaks related to H_3C –O–HF bending excitation, although these are not resolved experimentally.

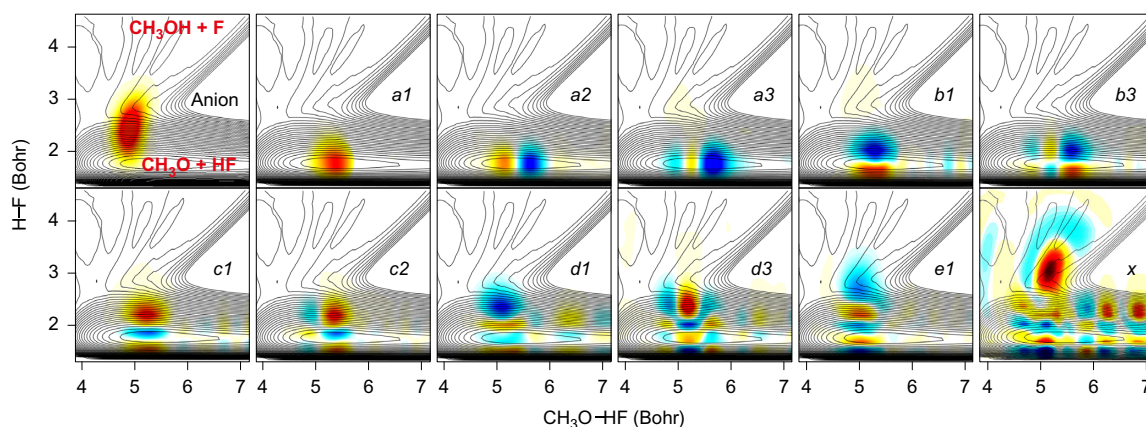


Figure 3 | Cuts of the CH_3OHF^- anion vibrational ground-state wavefunction and representative $\text{F} + \text{CH}_3\text{OH} \rightarrow \text{HF} + \text{CH}_3\text{O}$ resonance wavefunctions. The labels correspond to the related peaks in the simulated photodetachment spectrum of CH_3OHF^- (Fig. 2a). Wavefunctions are superimposed on the neutral PES contours plotted with respect to the $\text{CH}_3\text{O}-\text{HF}$ and $\text{H}-\text{F}$ bond distances with the other four coordinates relaxed. The locations of the entrance and exit channels are labelled in red in the upper-left plot. The $a1$, $b1$, $c1$, $d1$ and $e1$ wavefunctions are localized in the exit channel and demonstrate a growing number of nodes along the HF axis, which confirms that steps $a-e$ in Fig. 2 represent a progression of PC HF stretching states. The $a1$, $a2$ and $a3$ wavefunctions show a growing number of nodes along the $\text{CH}_3\text{O}-\text{HF}$ axis, which indicates that the finely spaced peaks correspond to vibrational progressions in the stretching mode between the product fragments.

The vibrational assignments made here are also sensible in the context of the Franck–Condon principle. Comparison of the anion and PC geometries (Supplementary Figs 2 and 3) indicates that photodetachment to the PC well should be accompanied by vibrational excitation in the HF stretching and the $\text{CH}_3\text{O}-\text{HF}$ stretching and bending modes. Indeed, the HF bond length in the anion (1.32 Å) is considerably longer than that of free HF (0.92 Å). The geometry of the methyl moiety is largely unchanged by detachment, so freezing its internal degrees of freedom during the quantum dynamical calculations does not have an adverse impact on the accuracy of the simulation. In this regard, the TS spectrum of $\text{F} + \text{CH}_3\text{OH}$ is analogous to that predicted and observed for the $\text{F} + \text{H}_2\text{O}$ system^{34,55}. In $\text{F} + \text{H}_2\text{O}$, photodetachment predominantly accesses the $\text{OH} + \text{HF}$ product well and is accompanied by considerable HF vibrational excitation, with the OH fragment acting as a spectator, as CH_3O does here.

We do not find evidence of resonances supported by the RC well. All sharp features that fall below the reactant asymptote (marked with a filled diamond in Fig. 2a) have wavefunctions localized on the product side of the TS (Fig. 3). Ray *et al.*²¹ tentatively assigned a spectral feature that lies below the reactant asymptote to an RC resonance, as it appeared to have a longer lifetime than neighbouring peaks. In the cryo-SEVI spectra this feature is resolved as peaks $d4$, $d5$ and $d6$, which are well-reproduced by theory as resonances in the PC well. On the other hand, the long-lived feature observed by Ray *et al.*²¹ represents a sufficiently small fraction of the total dissociative signal that there may not be a reasonable expectation of resolving it in our present experiment. Furthermore, such a state may not be captured accurately by our simulations as the reduced-dimensional model, which is ideal for the $\text{HF} + \text{CH}_3\text{O}$ product channel, might not be sufficient for the $\text{F} + \text{CH}_3\text{OH}$ reactant channel.

The resonances we report here are non-reactive as they are submerged below the energy of the free reactants. These states cannot, for instance, be accessed in an $\text{F} + \text{CH}_3\text{OH}$ scattering experiment and are therefore uniquely accessible with anion photoelectron spectroscopy. It is expected that reactive resonances also exist at higher energies, similar to the predictions for $\text{F} + \text{H}_2\text{O}$ (refs 34,55). The lowest-lying reactive resonance that is predicted theoretically underlies the feature labelled x in Fig. 2a. The wavefunction for this feature is shown in Fig. 3 and clearly has an intensity that extends into the reactant channel. Unfortunately, no

unambiguous evidence of this feature is resolved experimentally, as the spectrum becomes congested at higher photon energies.

The poor agreement between the experimental and theoretical results for the position and intensity of peak $e1$ could also be caused by experimental congestion. The laser-noise background becomes a limiting factor at high photon energies. It is also possible that detachment to excited $\text{F} + \text{CH}_3\text{OH}$ surfaces, analogous to those predicted in $\text{F} + \text{H}_2\text{O}$ (ref. 55), contributes at higher eBE, and leads to the increased baseline of the experimental spectra compared with theory. Additionally, the Wigner threshold law⁵⁶ can distort relative peak intensities close to the threshold, which may further hamper our ability to resolve peaks $e1$ and x at the relatively low electron kinetic energies accessible here.

In conclusion, we investigated the photodetachment of CH_3OHF^- and its singly deuterated isotopologue using slow photoelectron velocity-map imaging spectroscopy and quantum dynamical calculations on a new *ab initio* based PES. The cryo-SEVI spectrum is dominated by Feshbach resonances supported in the product well of the $\text{F} + \text{CH}_3\text{OH} \rightarrow \text{HF} + \text{CH}_3\text{O}$ reaction. These resonances are fully reproduced by theory, which allows their unambiguous assignment to the vibrational HF and $\text{CH}_3\text{O}-\text{HF}$ stretching states of the PC. This work demonstrates the utility of cryo-SEVI TS spectroscopy experiments for probing detailed multidimensional dynamical features near the TS as well as theoretical advances in modelling the dynamics of increasingly complex bimolecular reactions. It also illustrates that, despite much increased complexity, the key dynamical features of this seven-atom reaction remain largely local and can still be captured by a relatively simple physical picture.

Methods

The cryo-SEVI method has been described in detail elsewhere^{15–17}. CH_3OHF^- and CH_3ODF^- anions are prepared by expanding trace NF_3 and either methanol or methanol- d_1 vapour in helium gas through an Even–Lavie pulsed valve⁵⁷ fitted with a circular filament ionizer. Dissociative electron attachment to NF_3 produces F^- atomic ions, which then cluster with methanol($-d_1$). The anions are cooled by collisions with an 80:20 He:H₂ buffer gas mixture in a radiofrequency ion trap held at 5 K. After thermalization to their ground vibrational and electronic states, the ions are extracted from the trap and mass-selected by time-of-flight. The ions are photodetached at various photon energies with tunable light from the frequency-doubled output of a dye laser pumped by either the second or third harmonic of a neodymium:yttrium–aluminium–garnet laser. The electron kinetic energy distribution of the resulting photoelectrons is measured with a velocity-map imaging spectrometer⁵⁸ using relatively low extraction voltages. This magnifies the electron image on the detector and achieves a 1 cm^{-1} instrumental energy resolution for slow electrons¹⁸.

The quantum dynamical calculations are performed with a reduced-dimensional model, in which the methyl moiety is fixed at the geometry associated with the PC well. This is a reasonable approximation as the methyl group behaves largely as a spectator in the $F + CH_3OH \rightarrow HF + CH_3O$ channel. The remaining six coordinates are represented by the diatom–diatom Jacobi coordinates, in the same fashion as in our recent work on $F^-(H_2O)$ photodetachment⁵⁵. The photodetachment process is simulated within the Condon approximation, in which the anion wavefunction is placed on the neutral PES in a vertical transition. The subsequent dynamics are followed by propagating the initial wave packet in the Chebyshev order domain and the photoelectron spectrum is computed by a discrete cosine transform of the Chebyshev autocorrelation function⁵⁹. Additional theoretical details, including descriptions of the benchmark calculations and the construction of the PESs, are given in the Supplementary Information.

Data availability. The experimental and theoretical data that support the findings of this study are available from the corresponding authors on reasonable request.

Received 13 March 2017; accepted 19 May 2017;
published online 10 July 2017

References

- Herschbach, D. R. Reactive collisions in crossed molecular beams. *Discuss. Faraday Soc.* **33**, 149–161 (1962).
- Lee, Y. T., McDonald, J. D., LeBreton, P. R. & Herschbach, D. R. Molecular beam reactive scattering apparatus with electron bombardment detector. *Rev. Sci. Instrum.* **40**, 1402–1408 (1969).
- Levine, R. D. *Molecular Reaction Dynamics* (Cambridge Univ. Press, 2005).
- Eyring, H. The activated complex in chemical reactions. *J. Chem. Phys.* **3**, 107–115 (1935).
- Truhlar, D. G., Garrett, B. C. & Klippenstein, S. J. Current status of transition-state theory. *J. Phys. Chem.* **100**, 12771–12800 (1996).
- Guo, H. & Liu, K. Control of chemical reactivity by transition-state and beyond. *Chem. Sci.* **7**, 3992–4003 (2016).
- Polanyi, J. C. & Zewail, A. H. Direct observation of the transition state. *Acc. Chem. Res.* **28**, 119–132 (1995).
- Zare, R. N. Laser control of chemical reactions. *Science* **279**, 1875–1879 (1998).
- Yang, T. *et al.* Extremely short-lived reaction resonances in $Cl + HD (\nu = 1) \rightarrow DCl + H$ due to chemical bond softening. *Science* **347**, 60–63 (2015).
- Liu, K. Vibrational control of bimolecular reactions with methane by mode, bond, and stereoselectivity. *Annu. Rev. Phys. Chem.* **67**, 91–111 (2016).
- Neumark, D. M. Probing the transition state with negative ion photodetachment: experiment and theory. *Phys. Chem. Chem. Phys.* **7**, 433–442 (2005).
- Kim, J. B. *et al.* Spectroscopic observation of resonances in the $F + H_2$ reaction. *Science* **349**, 510–513 (2015).
- Ervin, K. M., Ho, J. & Lineberger, W. C. A study of the singlet and triplet states of vinylidene by photoelectron spectroscopy of H_2CC^+ , D_2CC^+ and $HDCC^+$. Vinylidene–acetylene isomerization. *J. Chem. Phys.* **91**, 5974–5992 (1989).
- Wenthold, P. G., Hrovat, D. A., Borden, W. T. & Lineberger, W. C. Transition-state spectroscopy of cyclooctatetraene. *Science* **272**, 1456–1459 (1996).
- Osterwalder, A., Nee, M. J., Zhou, J. & Neumark, D. M. High resolution photodetachment spectroscopy of negative ions via slow photoelectron imaging. *J. Chem. Phys.* **121**, 6317–6322 (2004).
- Neumark, D. M. Slow electron velocity-map imaging of negative ions: applications to spectroscopy and dynamics. *J. Phys. Chem. A* **112**, 13287–13301 (2008).
- Hock, C., Kim, J. B., Weichman, M. L., Yacovitch, T. I. & Neumark, D. M. Slow photoelectron velocity-map imaging spectroscopy of cold negative ions. *J. Chem. Phys.* **137**, 244201 (2012).
- Weichman, M. L., DeVine, J. A., Levine, D. S., Kim, J. B. & Neumark, D. M. Isomer-specific vibronic structure of the 9-, 1-, and 2-anthracenyl radicals via slow photoelectron velocity-map imaging. *Proc. Natl Acad. Sci. USA* **113**, 1698–1705 (2016).
- DeVine, J. A. *et al.* Non-adiabatic effects on excited states of vinylidene observed with slow photoelectron velocity-map imaging. *J. Am. Chem. Soc.* **138**, 16417–16425 (2016).
- Bradforth, S. E., Arnold, D. W., Metz, R. B., Weaver, A. & Neumark, D. M. Spectroscopy of the transition state: hydrogen abstraction reactions of fluorine. *J. Phys. Chem.* **95**, 8066–8078 (1991).
- Ray, A. W., Agarwal, J., Shen, B. B., Schaefer, H. F. & Continetti, R. E. Energetics and transition-state dynamics of the $F + HOCH_3 \rightarrow HF + OCH_3$ reaction. *Phys. Chem. Chem. Phys.* **18**, 30612–30621 (2016).
- Schatz, G. C., Bowman, J. M. & Kuppermann, A. Exact quantum, quasiclassical, and semiclassical reaction probabilities for the collinear $F + H_2 \rightarrow FH + H$ reaction. *J. Chem. Phys.* **63**, 674–684 (1975).
- Wyatt, R. E. & Redmon, M. J. Quantum-mechanical differential reaction cross sections for the $F + H_2 (\nu = 0) \rightarrow FH (\nu' = 2,3) + H$ reaction. *Chem. Phys. Lett.* **96**, 284–288 (1983).
- Schatz, G. C. Detecting resonances. *Science* **288**, 1599–1600 (2000).
- Zare, R. N. Resonances in reaction dynamics. *Science* **311**, 1383–1385 (2006).
- Liu, K. Quantum dynamical resonances in chemical reactions: from $A + BC$ to polyatomic systems. *Adv. Chem. Phys.* **149**, 1–46 (2012).
- Neumark, D. M., Wodtke, A. M., Robinson, G. N., Hayden, C. C. & Lee, Y. T. Molecular beam studies of the $F + H_2$ reaction. *J. Chem. Phys.* **82**, 3045–3066 (1985).
- Skodje, R. T. *et al.* Observation of a transition state resonance in the integral cross section of the $F + HD$ reaction. *J. Chem. Phys.* **112**, 4536–4552 (2000).
- Qiu, M. *et al.* Observation of Feshbach resonances in the $F + H_2 \rightarrow HF + H$ reaction. *Science* **311**, 1440–1443 (2006).
- Ren, Z., Sun, Z., Zhang, D. & Yang, X. A review of dynamical resonances in $A + BC$ chemical reactions. *Rep. Prog. Phys.* **80**, 026401 (2017).
- Russell, C. L. & Manolopoulos, D. E. How to observe the elusive resonances in $F + H_2$ reactive scattering. *Chem. Phys. Lett.* **256**, 465–473 (1996).
- Grand, E., Zhou, J., Manolopoulos, D. E., Alexander, M. H. & Neumark, D. M. Nonadiabatic interactions in the $Cl + H_2$ reaction probed by ClH_2^- and ClD_2^- photoelectron imaging. *Science* **319**, 72–75 (2008).
- Waller, I. M., Kitsopoulos, T. N. & Neumark, D. M. Threshold photodetachment spectroscopy of the $I + HI$ transition-state region. *J. Phys. Chem.* **94**, 2240–2242 (1990).
- Otto, R. *et al.* Imaging dynamics on the $F + H_2O \rightarrow HF + OH$ potential energy surfaces from wells to barriers. *Science* **343**, 396–399 (2014).
- Westermann, T. *et al.* Resonances in the entrance channel of the elementary chemical reaction of fluorine and methane. *Angew. Chem. Int. Ed.* **53**, 1122–1126 (2014).
- Active Thermochemical Tables Values based on v. 1.118 of the Thermochemical Network* (Argonne National Laboratory 2015); <http://ATcT.anl.gov>
- Feng, H., Randall, K. R. & Schaefer, H. F. Reaction of a fluorine atom with methanol: potential energy surface considerations. *J. Phys. Chem. A* **119**, 1636–1641 (2015).
- Glauser, W. A. & Koszykowski, M. L. Anomalous methoxy radical yields in the fluorine + methanol reaction. 2. Theory. *J. Phys. Chem.* **95**, 10705–10713 (1991).
- Jodkowski, J. T., Rayez, M.-T., Rayez, J.-C., Bérces, T. & Dóbe, S. Theoretical study of the kinetics of the hydrogen abstraction from methanol. 1. Reaction of methanol with fluorine atoms. *J. Phys. Chem. A* **102**, 9219–9229 (1998).
- Meier, U., Grotheer, H. H. & Just, T. Temperature dependence and branching ratio of the $CH_3OH + OH$ reaction. *Chem. Phys. Lett.* **106**, 97–101 (1984).
- Wickramaarachchi, M. A., Setser, D. W., Hildebrandt, H., Kórbitzer, B. & Heydtmann, H. Evaluation of HF product distributions deduced from infrared chemiluminescence. II. F atom reactions. *Chem. Phys.* **94**, 109–129 (1985).
- Khatoun, T. & Hoyermann, K. The reactions of fluorine atoms with normal and deuterated methanols. *Ber. Bunsen-Ges. Phys. Chem.* **92**, 669–673 (1988).
- Durant, J. L. Anomalous methoxy radical yields in the fluorine + methanol reaction. 1. Experiment. *J. Phys. Chem.* **95**, 10701–10704 (1991).
- Dóbe, S., Bérces, T., Temps, F., Wagner, H. G. & Ziemer, H. Formation of methoxy and hydroxymethyl free radicals in selected elementary reactions. *25th Symp. Int. Combust. Proc.* **25**, 775–781 (1994).
- Wladkowski, B. D., East, A. L. L., Mihalick, J. E., Allen, W. D. & Brauman, J. I. The proton-transfer surface of CH_3OH^+ . *J. Chem. Phys.* **100**, 2058–2088 (1994).
- Sun, L., Song, K., Hase, W. L., Sena, M. & Riveros, J. M. Stationary points for the $OH^- + CH_3F \rightarrow CH_3OH + F^-$ potential energy surface. *Int. J. Mass Spectrom.* **227**, 315–325 (2003).
- Gonzales, J. M. *et al.* Definitive *ab initio* studies of model S_N2 reactions $CH_3X + F^-$ ($X = F, Cl, CN, OH, SH, NH_2, PH_2$). *Chem. Eur. J.* **9**, 2173–2192 (2003).
- Knizia, G., Adler, T. B. & Werner, H.-J. Simplified CCSD(T)-F12 methods: theory and benchmarks. *J. Chem. Phys.* **130**, 054104 (2009).
- Jiang, B., Li, J. & Guo, H. Potential energy surfaces from high fidelity fitting of *ab initio* points: the permutation invariant polynomial-neural network approach. *Int. Rev. Phys. Chem.* **35**, 479–506 (2016).
- Li, J., Li, Y. & Guo, H. Covalent nature of $X \cdots H_2O$ ($X = F, Cl, \text{ and } Br$) interactions. *J. Chem. Phys.* **138**, 141102 (2013).
- Manz, J., Meyer, R., Pollak, E. & Romelt, J. A new possibility of chemical bonding. vibrational stabilization of IHI. *Chem. Phys. Lett.* **93**, 184–187 (1982).
- Manz, J., Meyer, R. & Schor, H. H. R. Interplay of vibrational and van der Waals type bonding. *J. Chem. Phys.* **80**, 1562–1568 (1984).
- Fleming, D. G., Manz, J., Sato, K. & Takayanagi, T. Fundamental change in the nature of chemical bonding by isotopic substitution. *Angew. Chem. Int. Ed.* **53**, 13706–13709 (2014).
- Levine, R. D. & Wu, S. F. Resonances in reactive collisions: computational study of the $H + H_2$ collision. *Chem. Phys. Lett.* **11**, 557–561 (1971).
- Ma, J. & Guo, H. Reactive and nonreactive Feshbach resonances accessed by photodetachment of FH_2O^- . *J. Phys. Chem. Lett.* **6**, 4822–4826 (2015).
- Wigner, E. P. On the behavior of cross sections near thresholds. *Phys. Rev.* **73**, 1002–1009 (1948).
- Even, U., Jortner, J., Noy, D., Lavie, N. & Cossart-Magos, C. Cooling of large molecules below 1 K and He clusters formation. *J. Chem. Phys.* **112**, 8068–8071 (2000).

58. Eppink, A. T. J. B. & Parker, D. H. Velocity map imaging of ions and electrons using electrostatic lenses: application in photoelectron and photofragment ion imaging of molecular oxygen. *Rev. Sci. Instrum.* **68**, 3477–3484 (1997).
59. Guo, H. A time-independent theory of photodissociation based on polynomial propagation. *J. Chem. Phys.* **108**, 2466–2472 (1998).

Acknowledgements

This work is funded by the US Air Force Office of Scientific Research (Grants no. FA9550-16-1-0097 to D.M.N. and no. FA9550-15-1-0305 to H.G.), and the National Natural Science Foundation of China (Contracts no. 21573027 to J.L. and no. 91441107 to J.M.). M.L.W. thanks the National Science Foundation for a graduate research fellowship.

Author contributions

The experimental research was conceived and supervised by D.M.N. The experiments were carried out by M.L.W., J.A.D. and M.C.B. Experimental data analysis and interpretation

was performed by M.L.W. Theoretical calculations were conceived by J.L., J.M. and H.G. and performed by J.L., L.G. and J.M. The paper was written by M.L.W., with the theoretical sections contributed by J.L., J.M. and H.G. All of the authors contributed to discussions about the results and manuscript.

Additional information

Supplementary information is available in the [online version of the paper](#). Reprints and permissions information is available online at www.nature.com/reprints. Publisher's note: Springer Nature remains neutral with regard to jurisdictional claims in published maps and institutional affiliations. Correspondence and requests for materials should be addressed to J.L. and D.M.N.

Competing financial interests

The authors declare no competing financial interests.